

## CHAPTER 4

### RESULTS AND DISCUSSION

#### 4.1 Structure elucidation of isolated compounds

In this investigation, some of biological activity of *O. paniculata* has been tested in which; dichloromethane and methanol extract were assay for their activity. The active dichloromethane extract was carried out for separation, purification and structure explanation (5 isolated compounds; eugenol (**22**), the mixture of  $\beta$ -sitosterol (**23**) and stigmasterol (**24**) along with, stigmastan-3,6-dione (**25**) and 3-acetylaleuritic acid (**26**)). The structures of all compounds were determined on the basis of spectral data such as  $^1\text{H}$  NMR,  $^{13}\text{C}$  NMR, COSY, DEPT, HMQC, HMBC, IR spectroscopy and mass spectrometry. The spectroscopic data were compared to the previously literature values.

Eugenol (**22**) (Figure 6), 4-allyl-2-methoxyphenol for a systematic name, which is brownish oil. It was isolated from fraction OPDF3 of the dichloromethane extract of *O. paniculata* twigs. The IR spectra data clearly indicated the appearance absorption of hydroxyl group at  $3418\text{ cm}^{-1}$ , C–O–C linkage of ether around  $1030\text{ cm}^{-1}$ , strong absorptions at  $1610$  and  $1510\text{ cm}^{-1}$  were also found from eugenol due to terminal double bond and aromatic moiety. The estimation of molecular weight at  $m/z$  165 [ $\text{M}^+$ ] which agreed with the molecular formula  $\text{C}_{10}\text{H}_{12}\text{O}_2$ . [22-24, 27] Fragmentation of eugenol (**22**) was indicated in Figure 12 compared with previous study. [30, 31]

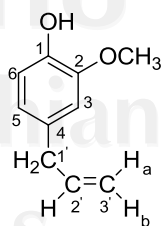


**Figure 6** Labelling number of each carbon in structure of eugenol (**22**)

The structure of eugenol (**22**) was elucidated by spectroscopic techniques mainly  $^1\text{H}$  NMR,  $^{13}\text{C}$  NMR, DEPT, COSY, HMQC, HMBC, MS and IR (Figure 7-12, Table 4 and 5). The 400 MHz ( $^1\text{H}$  NMR) and 100 MHz ( $^{13}\text{C}$  NMR) in  $\text{CDCl}_3$  spectra of eugenol (**22**) showed the presence of 12 protons in the molecule.[25, 26] The presence of an aromatic protons at  $\delta$  6.88 (*d*, 1H,  $J = 8.5$  Hz), 6.70-6.72 (*m*, 2H) could be assigned to be 1,2,4-trisubstituted benzene, together with the singlet of methoxy proton at  $\delta$  3.88 (*s*, 3H) and proton of hydroxyl group at  $\delta$  5.59 (*br*, 1H). The doublet pattern at  $\delta$  3.35 (*d*, 2H-1',  $J = 6.7$  Hz) is attached to aromatic ring. The signal at  $\delta$  5.09-5.14 (*m*, 2H-3') suggested that was methylene proton of terminal double bond and further confirmed by  $^1\text{H}$ - $^1\text{H}$  COSY spectrum (Figure 9) of the H-2' and H-3', indicating the location of terminal double bond. The  $^{13}\text{C}$  NMR displayed of 10 carbon atoms which are corresponding to DEPT  $90^\circ$  and DEPT  $135^\circ$  (Figure 8).[25-28] It indicated three quaternary, four tertiary, two secondary and one methyl carbons. Notably, the chemical shift at 55.7 ppm was assigned to methoxy at *para* position of benzene ring. The downfield quaternary carbons at 143.84 and 146.39 ppm corresponded to aromatic carbon (C-1, C-2) bearing a hydroxyl and methoxy group while the upfield quaternary carbon (C-4) at 131.85 ppm was allylic group which confirmed by HMBC correlation (Figure 11). It showed the interactions between proton of methoxy group at 3.88 ppm to C-2, H-3 ( $\delta$  6.88) to C-1, C-2, C-4, C-5, C-6, H-1' ( $\delta$  3.55) to C-2', C-3', C-4, C-5, C-6 as shown in Table 5. Consequently, alkoxy group of 55.7 ppm and allylic group substantiated at C-2 ( $\delta$  146.3) and C-4 ( $\delta$  131.8). By further analysis of 2D data, HMQC correlation (Figure 10) showed the signals of 6.88 ppm (H-3), 5.93-6.04 ppm (H-2') and 3.88 ppm which correlated directly with C-3, C-2' and C-2, respectively. The structure of compound **22** was finally confirmed by directed comparison of  $^1\text{H}$  and  $^{13}\text{C}$  NMR with the value reported by Fujisawa *et al.*[28] and Toda *et al.*[29].

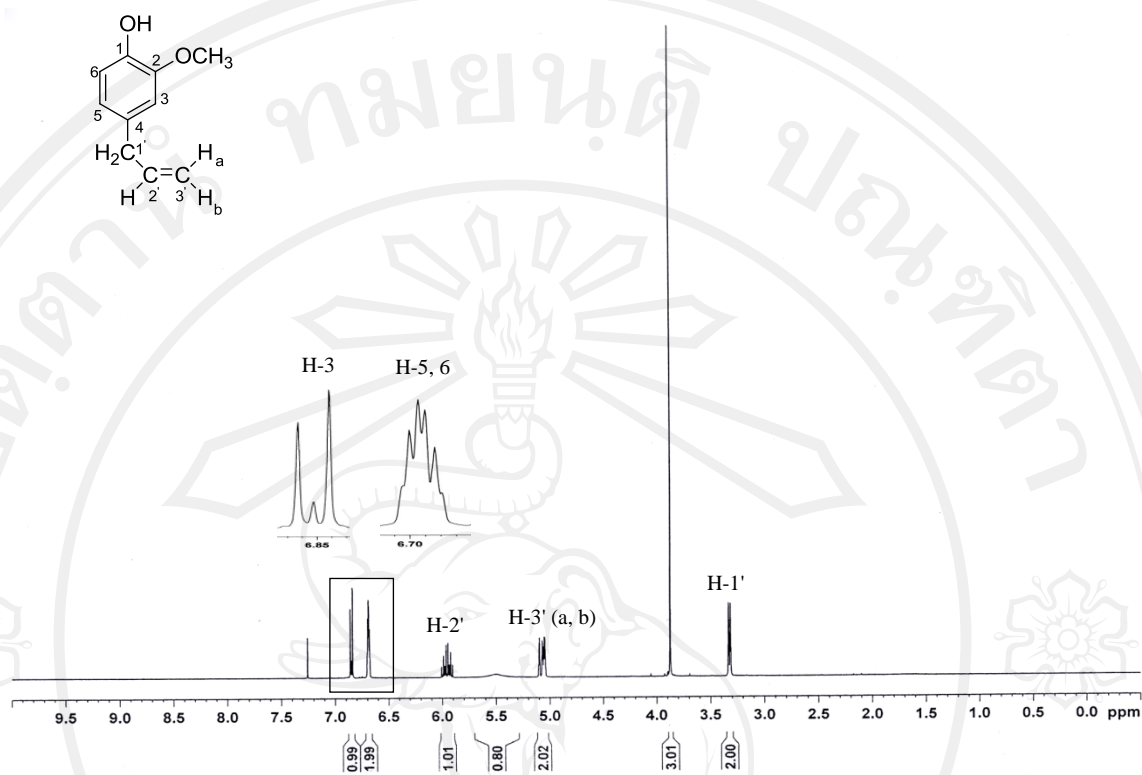


Figure 7  $^1\text{H}$  NMR spectrum of eugenol (22)

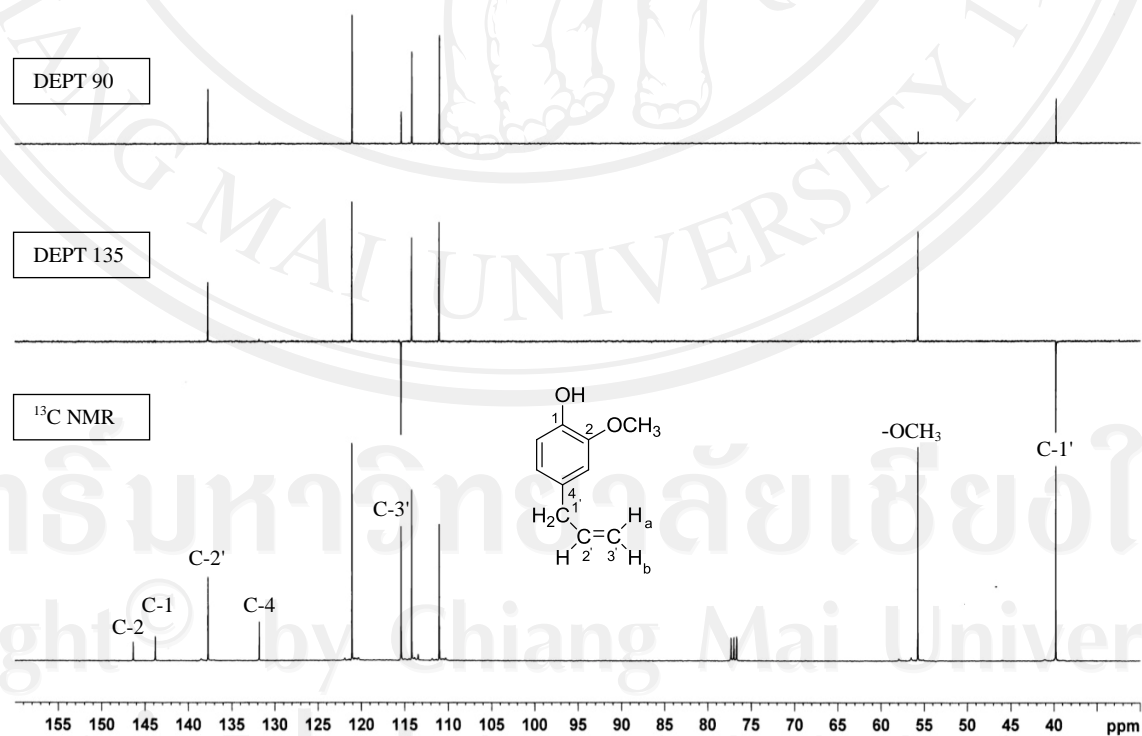


Figure 8 DEPT 90, DEPT 135 and  $^{13}\text{C}$  NMR spectra of eugenol (22)

**Table 3**  $^1\text{H}$  and  $^{13}\text{C}$  NMR data of eugenol (**22**) ( $\text{CDCl}_3$ ) at 400 ( $^1\text{H}$  NMR) and 100 MHz ( $^{13}\text{C}$  NMR)

Position	Chemical shift ( $\delta$ ) in ppm	
	$^1\text{H}$ NMR	$^{13}\text{C}$ NMR
1	-	143.8
2	-	146.3
3	6.88 [ <i>d</i> , 1H, <i>J</i> = 8.5 Hz]	114.2
4	-	131.8
5, 6	6.70-6.72 [ <i>m</i> , 1H]	111.0, 121.1
1'	3.35 [ <i>d</i> , 2H, <i>J</i> = 6.7 Hz]	39.8
2'	5.93-6.04 [ <i>m</i> , 1H]	137.7
3'	5.09-5.14 [ <i>m</i> , 2H],	115.4
O-CH <sub>3</sub>	3.88 [ <i>s</i> , 3H]	55.7
OH	5.59 [ <i>br</i> , 1H]	-

**Table 4**  $^1\text{H}$ - $^1\text{H}$  COSY, HMQC, HMBC data of eugenol (**22**) ( $\text{CDCl}_3$ ) at 400 MHz ( $^1\text{H}$  NMR) and 100 MHz ( $^{13}\text{C}$  NMR)

Proton position	$^1\text{H}$ - $^1\text{H}$ COSY (Coupling of H)	HMQC (Correlation of C)	HMBC (Correlation of C)
1	-	-	-
2	-	-	-
3	H-5, 6	C-3	C-1, 2, 4, 5, 6
4	-	-	-
5, 6	H-3	C-5, 6	C-1', 1, 2, 4
1'	H-3'	C-1'	C-3, 4, 5, 6, 2'
2'	H-1', 3'	C-2'	C-1', 4
3'	H-2'	C-3'	C-1', 2'
O-CH <sub>3</sub>	-	CH <sub>3</sub> -O	C-2
OH	-	-	-

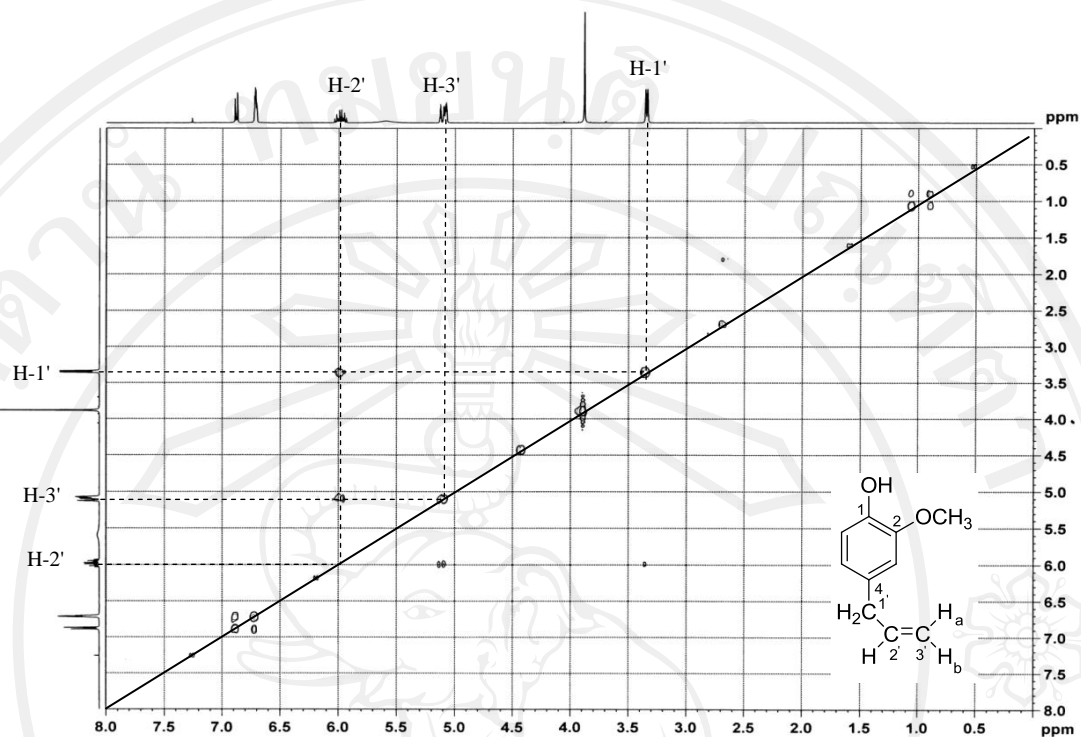


Figure 9  $^1\text{H}$ - $^1\text{H}$  COSY spectrum of eugenol (22)

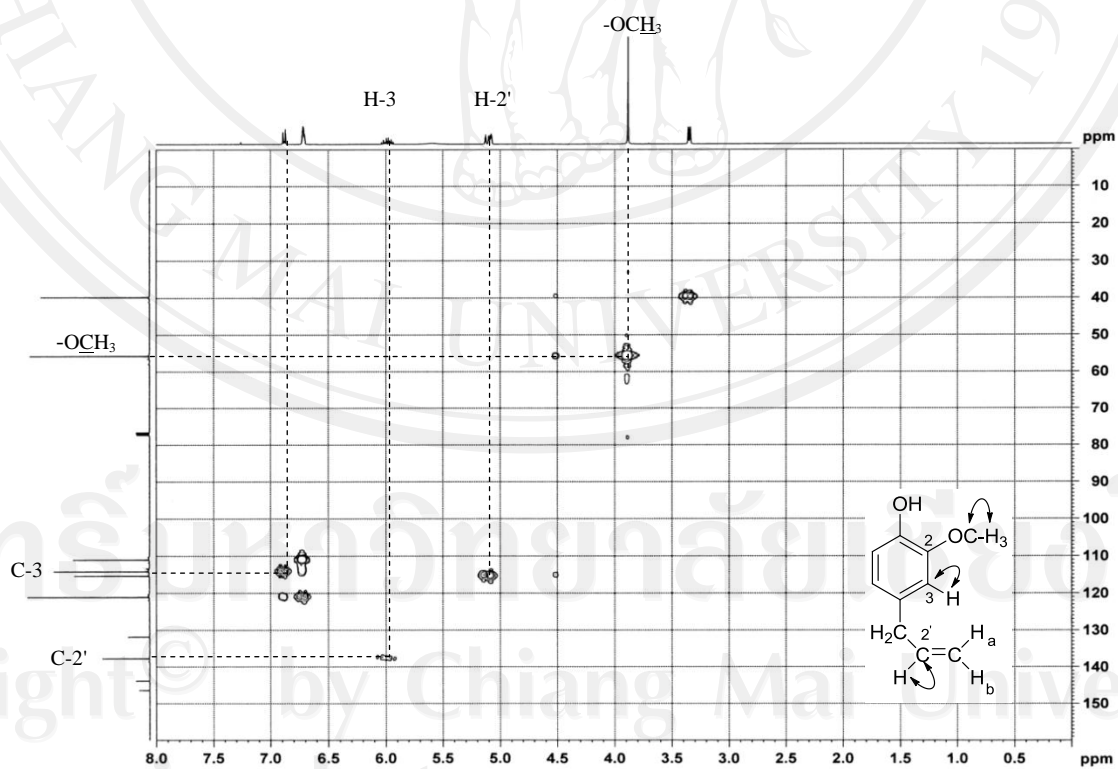
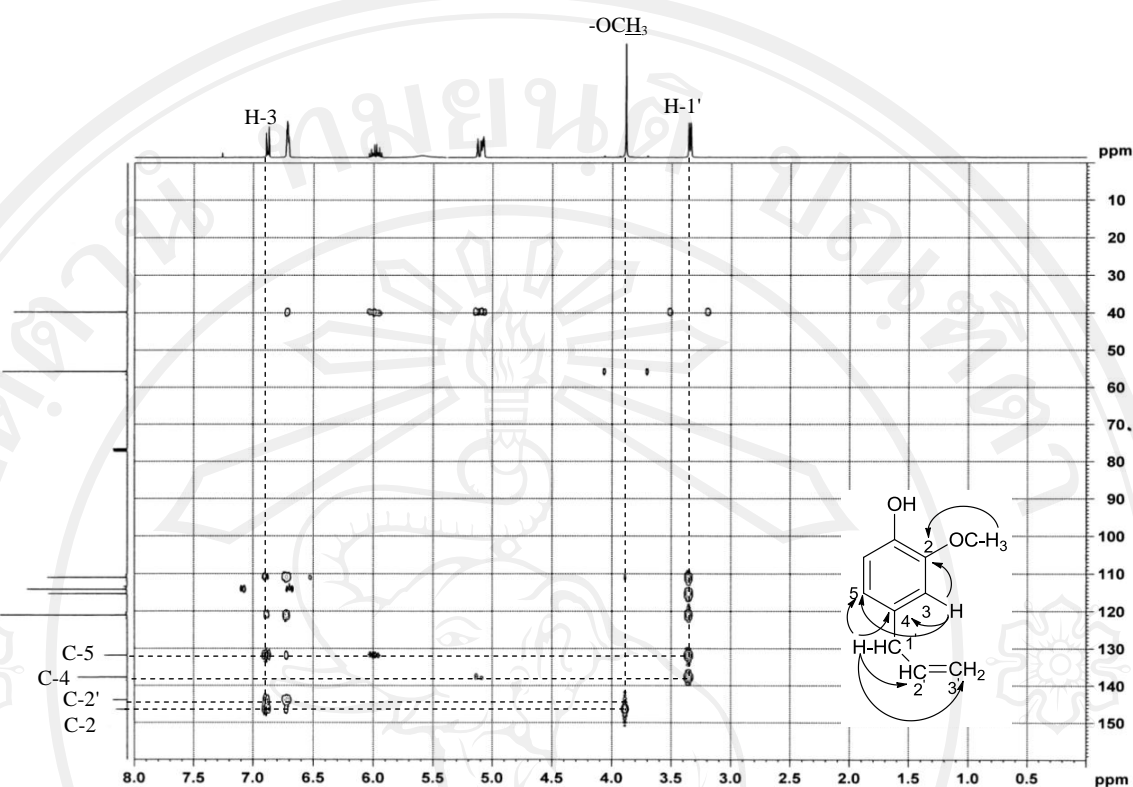
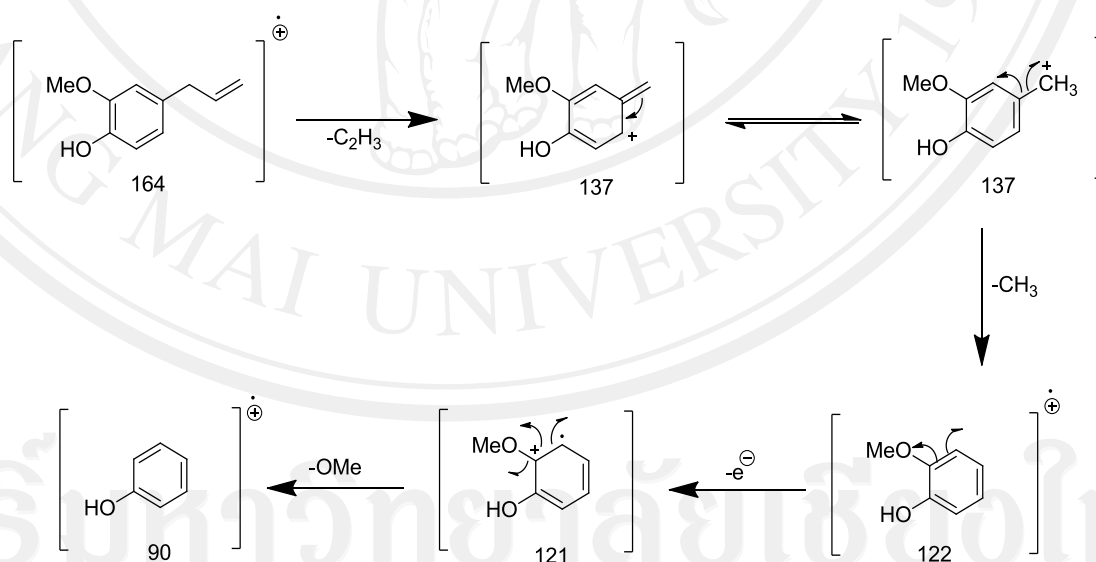


Figure 10 Selected HMQC correlation of eugenol (22)



**Figure 11** Selected HMBC correlation of eugenol (**22**)



**Figure 12** The fragmentation pathways for eugenol (**22**)

The structure of the mixture of phytosterol;  $\beta$ -sitosterol (**23**) and stigmasterol (**24**) were elucidated by spectroscopic techniques mainly  $^1\text{H}$  NMR,  $^{13}\text{C}$  NMR, MS and IR (Figure 13-16, Table 6 and 7). The mixture of  $\beta$ -sitosterol (**23**) and stigmasterol

(**24**) obtained as colorless crystals. Melting point was found in a range of 133 – 136 °C.[34, 35] The EI-MS spectrum of these mixture compounds manifested a molecular ion peak at 412 and 414, subsequently which corresponds to  $C_{29}H_{48}O$  and  $C_{29}H_{50}O$ . Explaining mechanism of their fragmentation is depicted in Figure 16.[33]

Its IR spectrum exhibited hydroxyl group around  $3390-3430\text{ cm}^{-1}$  and olefinyl moieties at  $1625\text{ cm}^{-1}$ . [31, 32] In the  $^1\text{H}$  NMR spectrum (Figure 14), the major difference signals were the presence of olefinic protons at 5.06 (*dd*, 1H,  $J = 8.6, 8.7$  Hz) and 5.19 (*dd*, 1H,  $J = 8.5, 8.6$  Hz) which assigned to H-22 and H-23 corresponded to C-22 (138.3) and C-23 (129.7) of stigmasterol.[27, 28] The others signals 5.35 (*d*, 1H,  $J = 5.2$  Hz) and 71.8 ppm were assigned to H-6 of both  $\beta$ -sitosterol and stigmasterol.[37-39] The integration areas of H-6, H-22 and H-23 appeared to be in the ratio of 1.02:0.37:0.28. By directed comparison, of  $^1\text{H}$  and  $^{13}\text{C}$  NMR data to the previously reported compound.[33] They could be deduced that the mixture of  $\beta$ -sitosterol and stigmasterol was in ratio of 78:22.

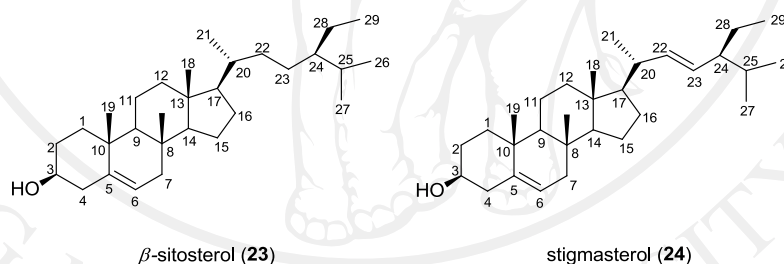


**Figure 13** Labelling number of each carbon in structure of  $\beta$ -sitosterol (**23**) and stigmasterol (**24**)

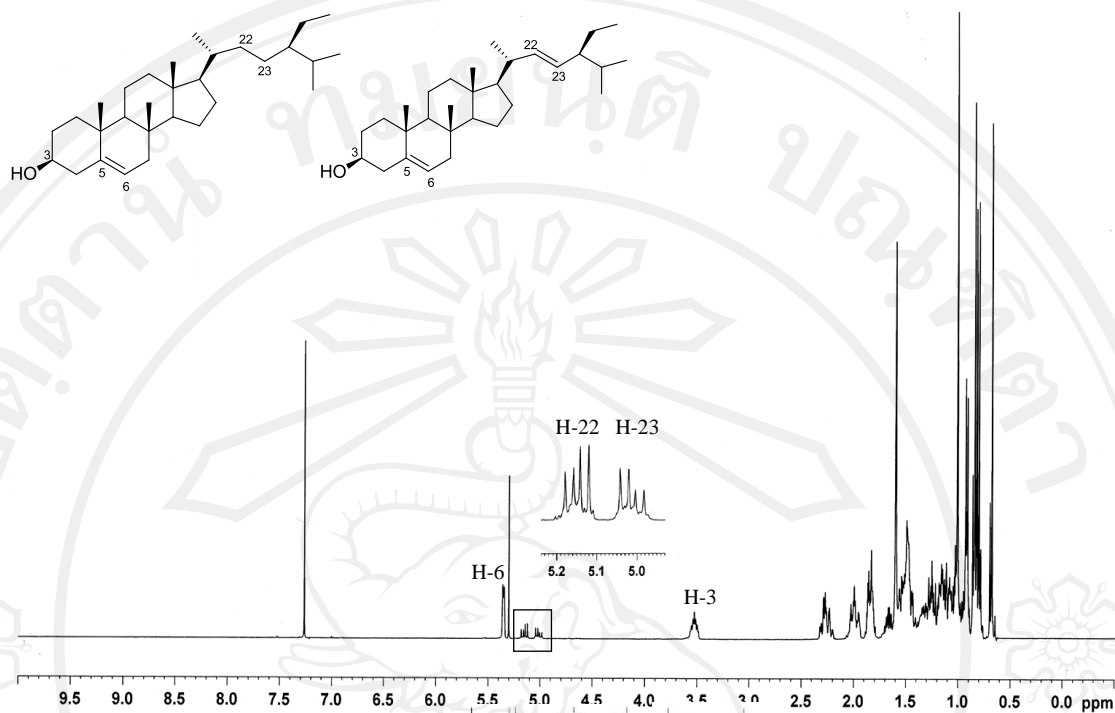


Figure 15  $^1\text{H}$  NMR spectrum of  $\beta$ -sitosterol (23) and stigmasterol (24)

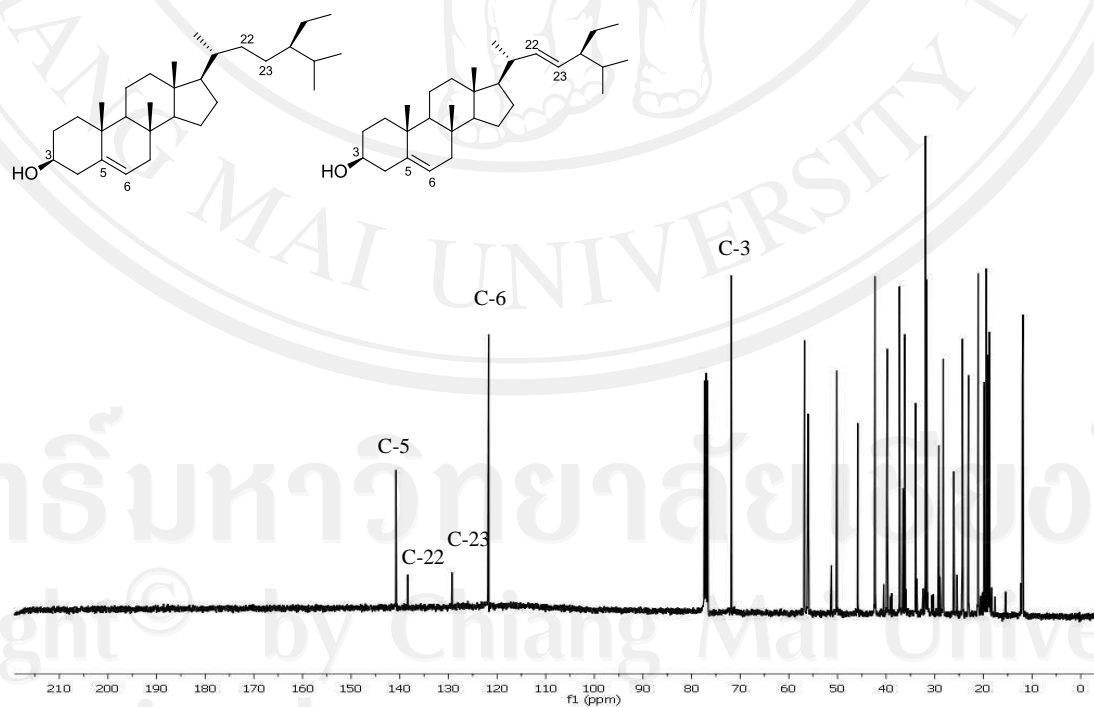


Figure 16  $^{13}\text{C}$  NMR spectrum of  $\beta$ -sitosterol (23) and stigmasterol (24)

**Table 5**  $^1\text{H}$  NMR data of  $\beta$ -sitosterol (**23**) and stigmasterol (**24**) ( $\text{CDCl}_3$ ) at 400 MHz

Chemical shift ( $\delta$ ) in ppm		
$^1\text{H}$ NMR (from experimental)	$^1\text{H}$ NMR (from reference)[37]	$ \Delta\delta_{\text{H}} (\text{ppm})$
0.71 [s]	0.71 [s]	0.00
0.68 [s]	0.73 [s]	0.05
0.84 [d, $J = 6.5$ Hz]	0.85[d, $J = 6.4$ Hz]	0.01
0.86 [d, $J = 1.5$ Hz]	0.86[d, $J = 6.8$ Hz]	0.00
0.92 [d, $J = 4.0$ Hz]	0.88[d, $J = 6.8$ Hz]	0.04
1.02 [s]	1.04[s]	0.02
1.05 [s]	1.06[s]	0.01
1.21-1.30 [m]	1.21-1.30 [m]	0.00
1.40-1.65 [m]	1.45-1.65 [m]	0.05
1.64-1.71 [m]	1.67-1.70 [m]	0.01
1.80-1.89 [m]	1.84-1.90 [m]	0.03
2.24-2.33 [m]	2.24-2.30 [m]	0.03
3.48-3.55 [m]	3.53-3.59 [m]	0.01

**Table 6**  $^{13}\text{C}$  NMR data of  $\beta$ -sitosterol (**23**) and stigmasterol (**24**) ( $\text{CDCl}_3$ ) at 100 MHz

Chemical shift ( $\delta$ ) in ppm		
$^{13}\text{C}$ NMR (from experimental)	$^{13}\text{C}$ NMR (from reference)[37]	$ \Delta\delta_{\text{C}} (\text{ppm})$
11.8-19.0	12.0-19.0	0.2
21.3-56.8	21.1- 56.8	0.2
71.9	71.8	0.1
121.7	121.7	0.0
129.7	129.1	0.6
138.3	138.2	0.1
140.7	140.8	0.1

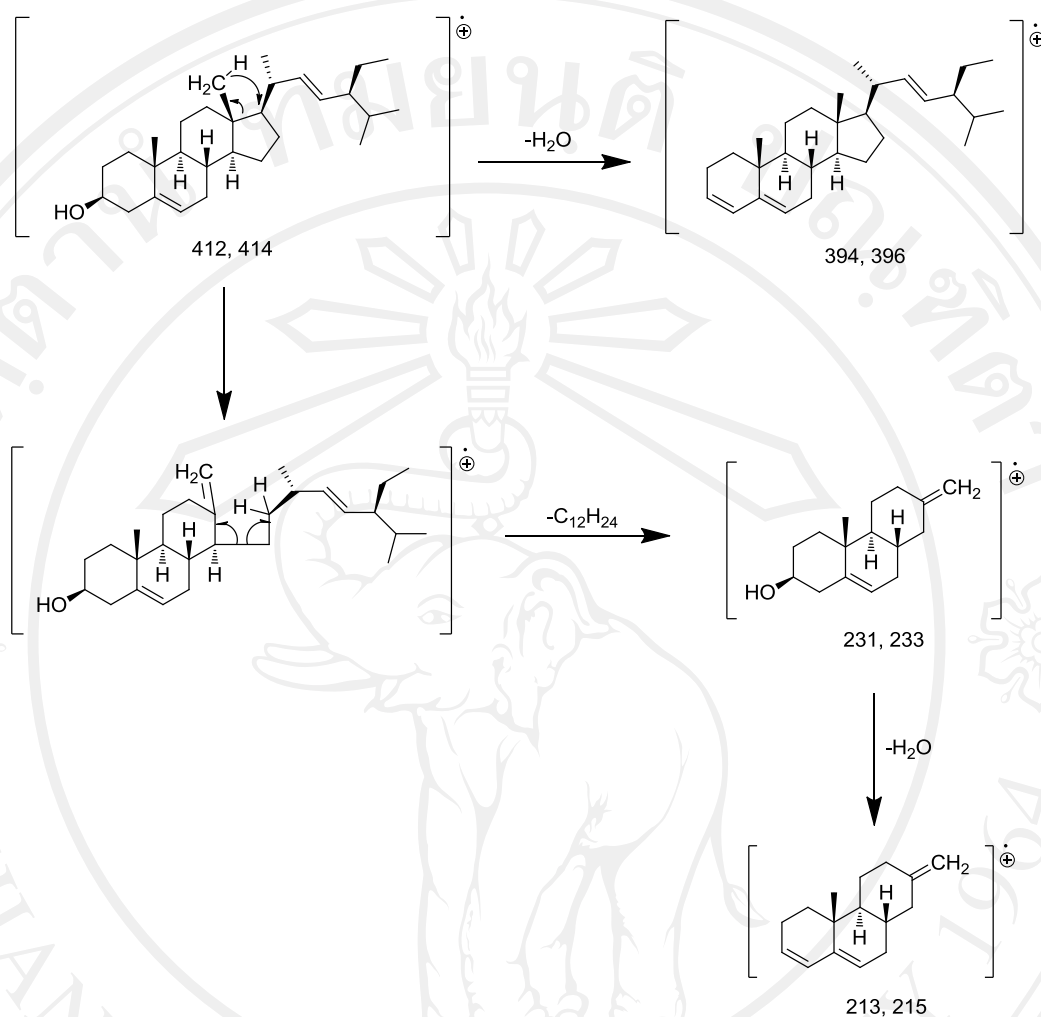


**Figure 16** The fragmentation pathways for  $\beta$ -sitosterol (**23**) and stigmasterol (**24**)

The structure of stigmastan-3,6-dione (**25**) (Figure 17) was elucidated by spectroscopic techniques mainly  $^1\text{H}$  NMR,  $^{13}\text{C}$  NMR, DEPT, COSY, HMQC, HMBC, MS and IR (Figure 18-23, Table 8 and 9). Stigmastan-3,6-dione (**25**); which called  $5\alpha$ -stigmastane-3,6-dione in the systematic name. It was a white amorphous crystal, mp  $192.0 - 194.0$  °C,  $[\alpha]_{\text{D}}^{29.3} +50.0^\circ$  which corresponding to  $\text{C}_{29}\text{H}_{48}\text{O}_2$  by means of EI-MS measurement on the  $[\text{M}^+]$  428.[39, 43] The probability of their fragmentation of compound **25** can describe with earlier report [40], as shown in Figure 23. Absorption bands of IR spectra associated with two ketonic in the region  $1716$  and  $1708$   $\text{cm}^{-1}$ . [39, 40]

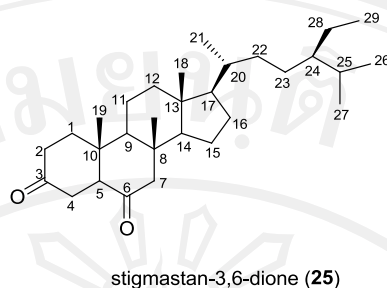


**Figure 17** Labelling number of each carbon in structure of stigmastan-3,6-dione (**25**)

Additionally, the  $^1\text{H}$  NMR (Figure 18) data are attributed to three active methylene groups of H-2, H-4, H-7 at 2.00-2.59 (*m*, 6H) and one methine proton at 2.59 (*m*, H-5) adjacent of two carbonyl groups which related with the interpretation of  $^1\text{H}$ - $^1\text{H}$  COSY spectrum (Figure 20). The signal at  $\delta$  2.33, 2.57 (H-2, 2H) showed correlation with signal proton at  $\delta$  2.36, 2.59 (H-4), 1.63 and 2.11 (H-1). At 2.59 ppm (H-5, 1H) showed the correlation with H-4 and H-7. In methyl region (0.69, 0.80, 0.84, 0.86, 0.92 and 0.95 ppm, 18H) assigned to the six methyl groups of two angular and four side-chain methyl.

The  $^{13}\text{C}$  NMR and DEPT spectra (Figure 19) displayed 29 carbon signals. Two carbonyl carbon of ketone at 211.2 (C-3), 209.1 (C-6), which were confirmed by the presence of the HMBC spectra (Figure 22). It displayed that the signal of methylene proton (H-1) at (1.63, 2.11 ppm) with C-2, C-3 and C-19, H-2 (2.33, 2.57 ppm) with C-1 and C-3, H-4 (2.36, 2.59 ppm) with C-2, C-5 and also H-5 (2.59 ppm) with C-4 and C-7. In  $^1\text{H}$ - $^{13}\text{C}$  directed correlation observed in HMQC (Figure 21) experiment verified that protons on C-2 position at 2.33 and 2.57 ppm were correlated with C-2, two protons on C-4 at 2.36 and 2.59 ppm had relationship with C-4 and proton on C-5 position at 2.59 ppm was bonded with C-5 that adjoined with two quaternary carbons of ketone group. From above the evidence, compound **25** was determined as stigmastan-3,6-dione as reported previously.[40-44]

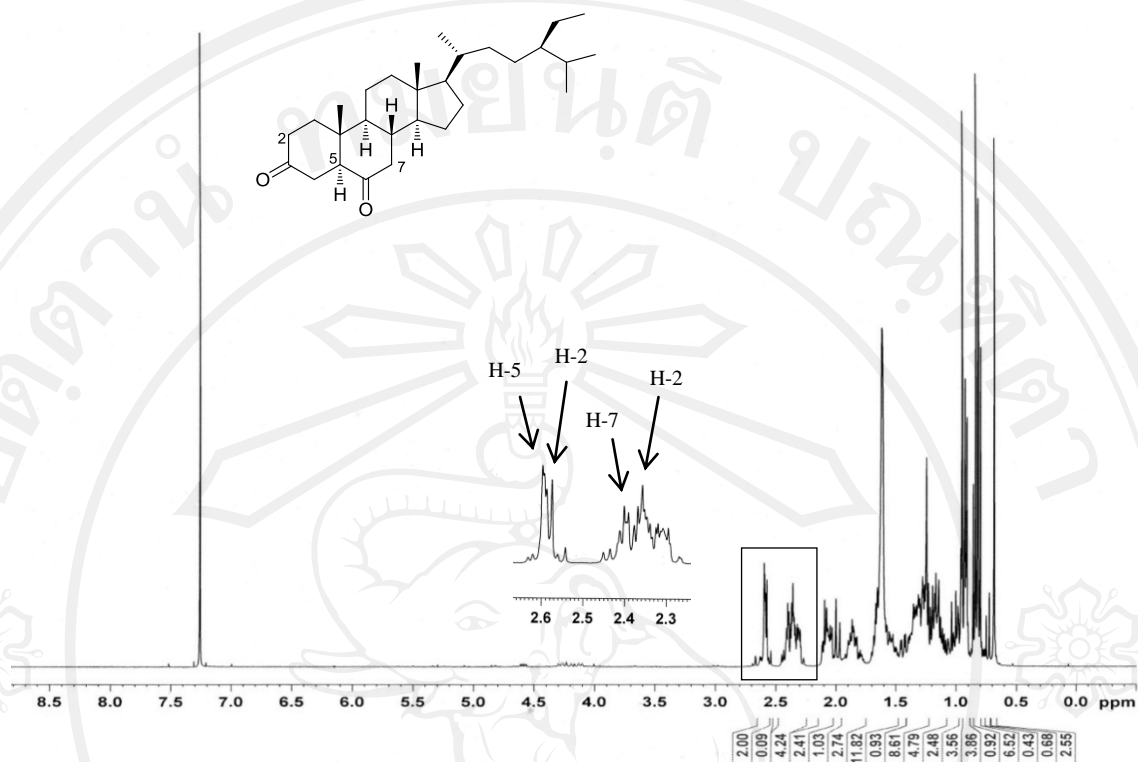


Figure 18  $^1\text{H}$  NMR spectrum of stigmastan-3,6-dione (25)

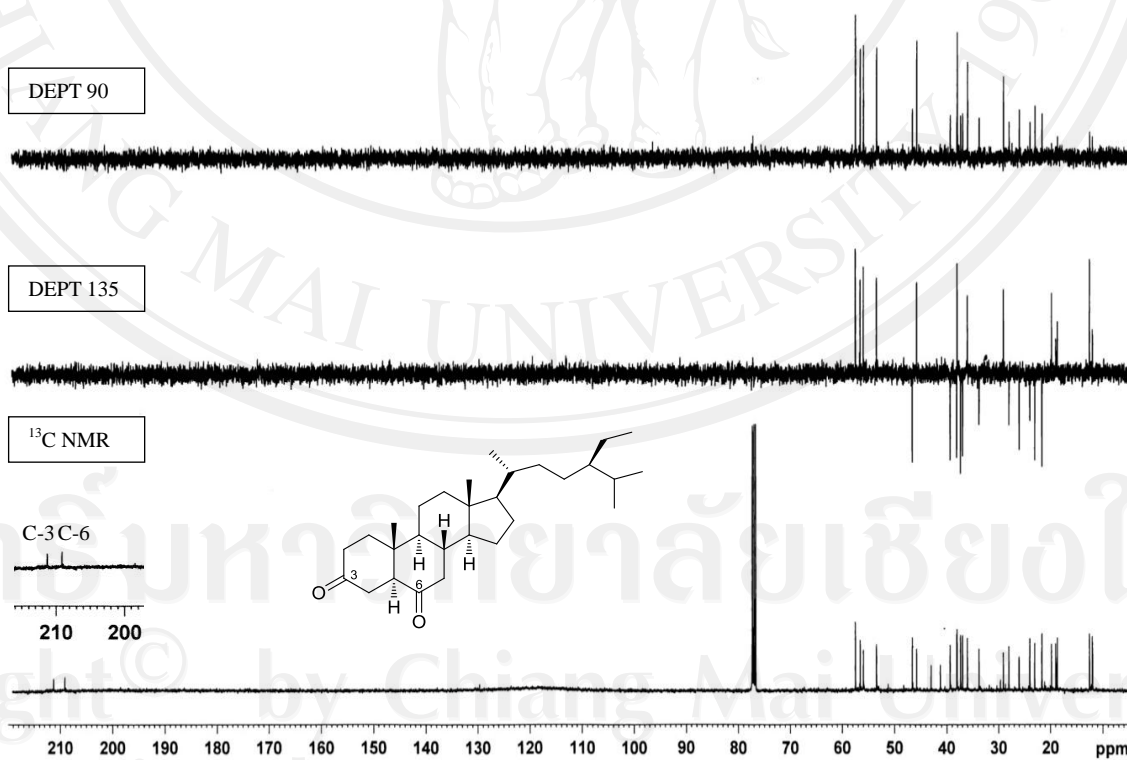


Figure 19 DEPT 90, DEPT 135 and  $^{13}\text{C}$  NMR spectra of stigmastan-3,6-dione (25)

**Table 7**  $^1\text{H}$  and  $^{13}\text{C}$  NMR data of stigmastan-3,6-dione (**25**) ( $\text{CDCl}_3$ ) at 400 MHz ( $^1\text{H}$  NMR) and 100 MHz ( $^{13}\text{C}$  NMR)

Position	Chemical shift ( $\delta$ ) In ppm	
	$^1\text{H}$ NMR	$^{13}\text{C}$ NMR
1	1.63, 2.11 [ <i>m</i> , 2H]	37.9
2	2.33, 2.57 [ <i>m</i> , 2H]	37.0
3	-	211.3
4	2.36, 2.59 [ <i>m</i> , 2H]	38.1
5	2.59 [ <i>m</i> , 1H]	57.5
6	-	209.3
7	2.00, 2.38 [ <i>m</i> , 2H]	46.6
8	1.85 [ <i>m</i> , 1H]	38.0
9	1.33 [ <i>m</i> , 1H]	53.5
10	-	41.3
11	1.42, 1.65 [ <i>m</i> , 2H]	21.7
12	1.25, 2.06 [ <i>m</i> , 2H]	56.0
13	-	24.0
14	1.25 [ <i>m</i> , 1H]	28.0
15	1.53 [ <i>m</i> , 2H]	24.0
16	1.31 [ <i>m</i> , 2H]	28.0
17	1.16 [ <i>m</i> , 1H]	56.6
18	0.69 [ <i>s</i> , 3H]	11.9
19	0.95 [ <i>s</i> , 3H]	12.6
20	1.37 [ <i>m</i> , 1H]	36.0
21	0.92 [ <i>d</i> , 3H, $J = 6.5$ Hz]	18.7
22	1.02, 1.34 [ <i>m</i> , 2H]	33.8
23	1.16 [ <i>m</i> , 2H]	26.1
24	0.92 [ <i>m</i> , 1H]	45.8
25	1.25 [ <i>m</i> , 1H]	29.1
26	0.84 [ <i>d</i> , 3H, $J = 6.5$ Hz]	19.8

**Table 7**  $^1\text{H}$  and  $^{13}\text{C}$  NMR data of stigmastan-3,6-dione (**25**) ( $\text{CDCl}_3$ ) at 400 MHz ( $^1\text{H}$  NMR) and 100 MHz ( $^{13}\text{C}$  NMR) (Cont.)

Position	Chemical shift ( $\delta$ ) in ppm	
	$^1\text{H}$ NMR	$^{13}\text{C}$ NMR
27	0.84 [ <i>d</i> , 3H, $J = 7.1$ Hz]	19.0
28	1.21, 1.28 [ <i>m</i> , 2H]	23.1
29	0.86 [ <i>t</i> , 3H, $J = 5.8, 7.7$ Hz]	12.0

**Table 8**  $^1\text{H}$ - $^1\text{H}$  COSY, HMQC, HMBC data of stigmastan-3,6-dione (**25**) ( $\text{CDCl}_3$ ) at 400 MHz ( $^1\text{H}$  NMR) and 100 MHz ( $^{13}\text{C}$  NMR)

Proton position	$^1\text{H}$ - $^1\text{H}$ COSY	HMQC	HMBC
	(Coupling of H)	(Correlation of C)	(Correlation of C)
1	H-2	C-1	C-2, 3, 19
2	H-1, 4	C-2	C-1, 3
3	-	-	-
4	H-2, 5	C-4	C-3, 4, 6, 10
5	H-4, 7	C-5	C-3, 6, 10
6	-	-	-
7	H-8	C-7	C-5, 6, 8, 9
8	H-7, 9, 14	C-8	C-7, 9, 11, 14
9	H-8, 11	C-9	C-8, 10, 11, 14
10	-	-	-
11	H-12	C-11	C-9, 12, 13, 19
12	H-11, 14	C-12	C-9, 11, 13
13	-	-	-
14	H-8, 12	C-14	C-8, 9, 13, 15
15	H-14, 17	C-15	C-14, 16, 17
16	-	-	-
17	H-15	C-17	C-16, 17, 18, 20
18	-	-	-

**Table 8**  $^1\text{H}$ - $^1\text{H}$  COSY, HMQC, HMBC data of stigmastan-3,6-dione (**25**) ( $\text{CDCl}_3$ ) at 400 MHz ( $^1\text{H}$  NMR) and 100 MHz ( $^{13}\text{C}$  NMR) (Cont.)

Proton position	$^1\text{H}$ - $^1\text{H}$ COSY (Coupling of H)	HMQC (Correlation of C)	HMBC (Correlation of C)
19	-	-	-
20	H-21, 22	C-20	C-23
21	H-20, 22	C-21	C-17, 20, 22
22	H-20, 23	C-22	C-21, 23
23	H-28	C-23	C-22, 24
24	H-22, 23	C-24	C-23, 25, 28
25	H-26, 27	C-25	C-24, 26, 27
26	H-25, 26	C-26	C-24, 28
27	H-25, 26	C-27	C-24, 25, 26
28	H-21	C-28	C-23, 24, 25, 29
29	H-25	C-29	C-24, 28

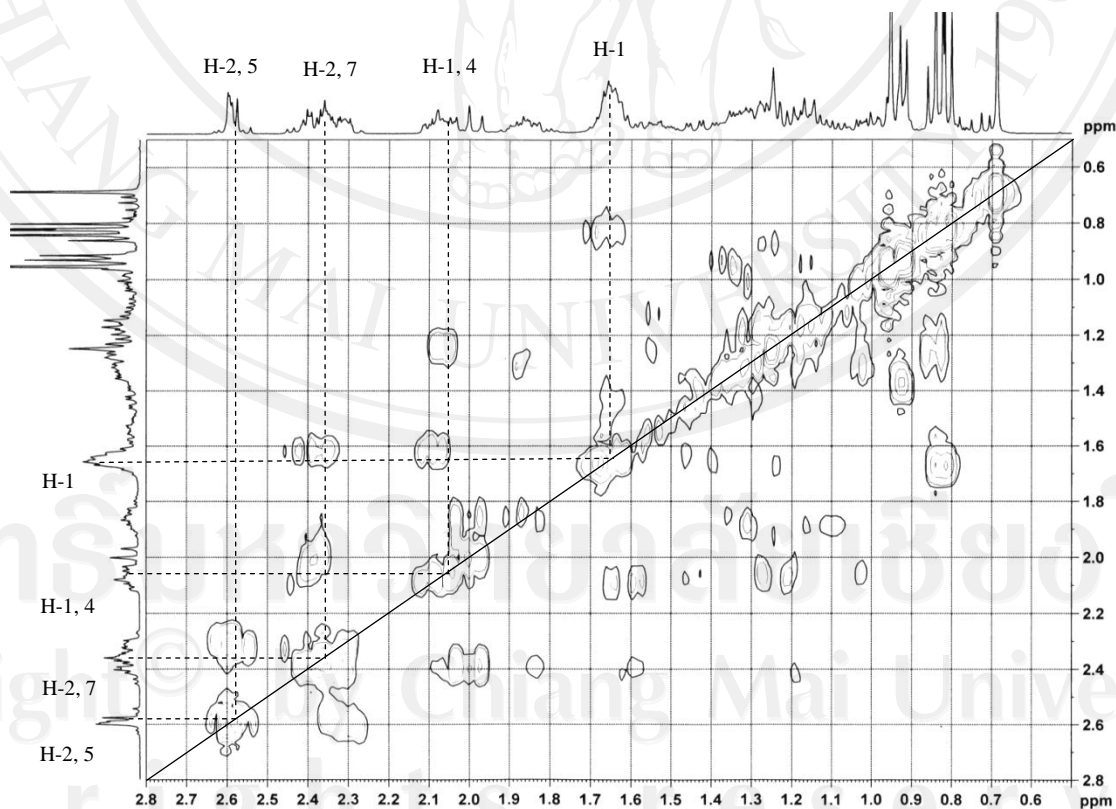


**Figure 20**  $^1\text{H}$ - $^1\text{H}$  COSY spectrum of stigmastan-3,6-dione (**25**)

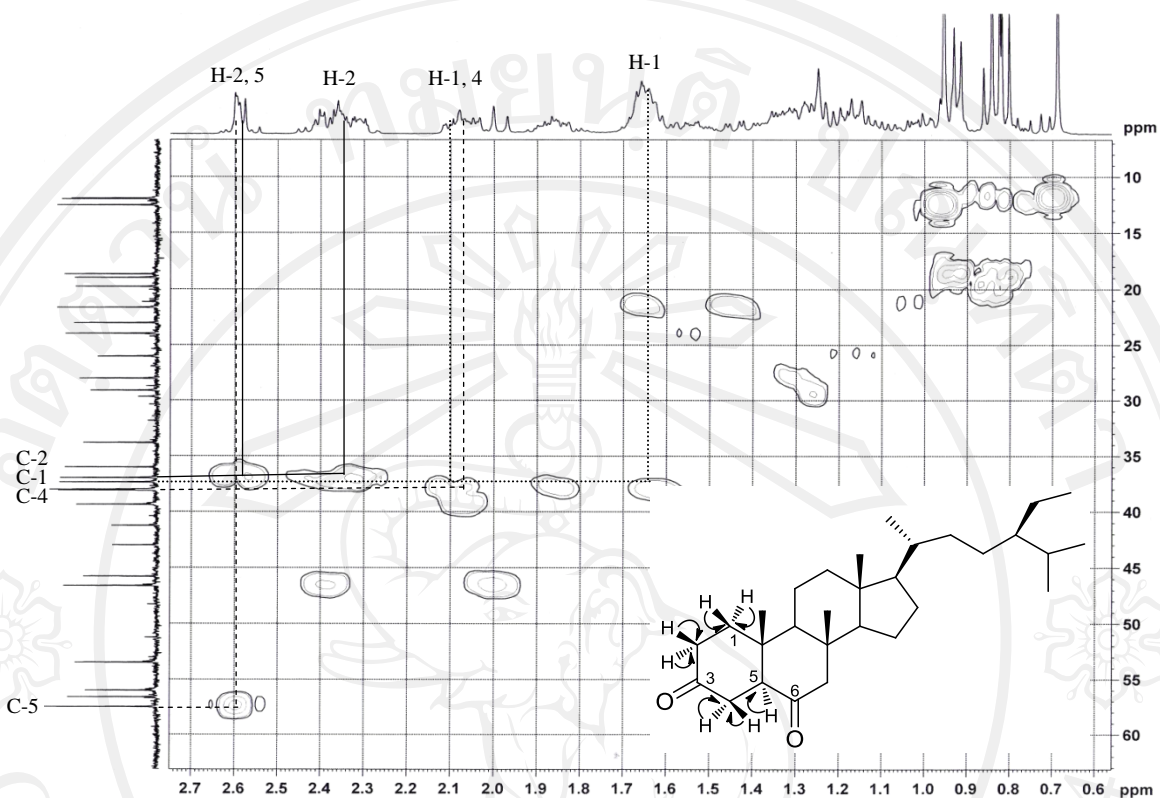


**Figure 21** Selected HMQC correlation of stigmastan-3,6-dione (25)

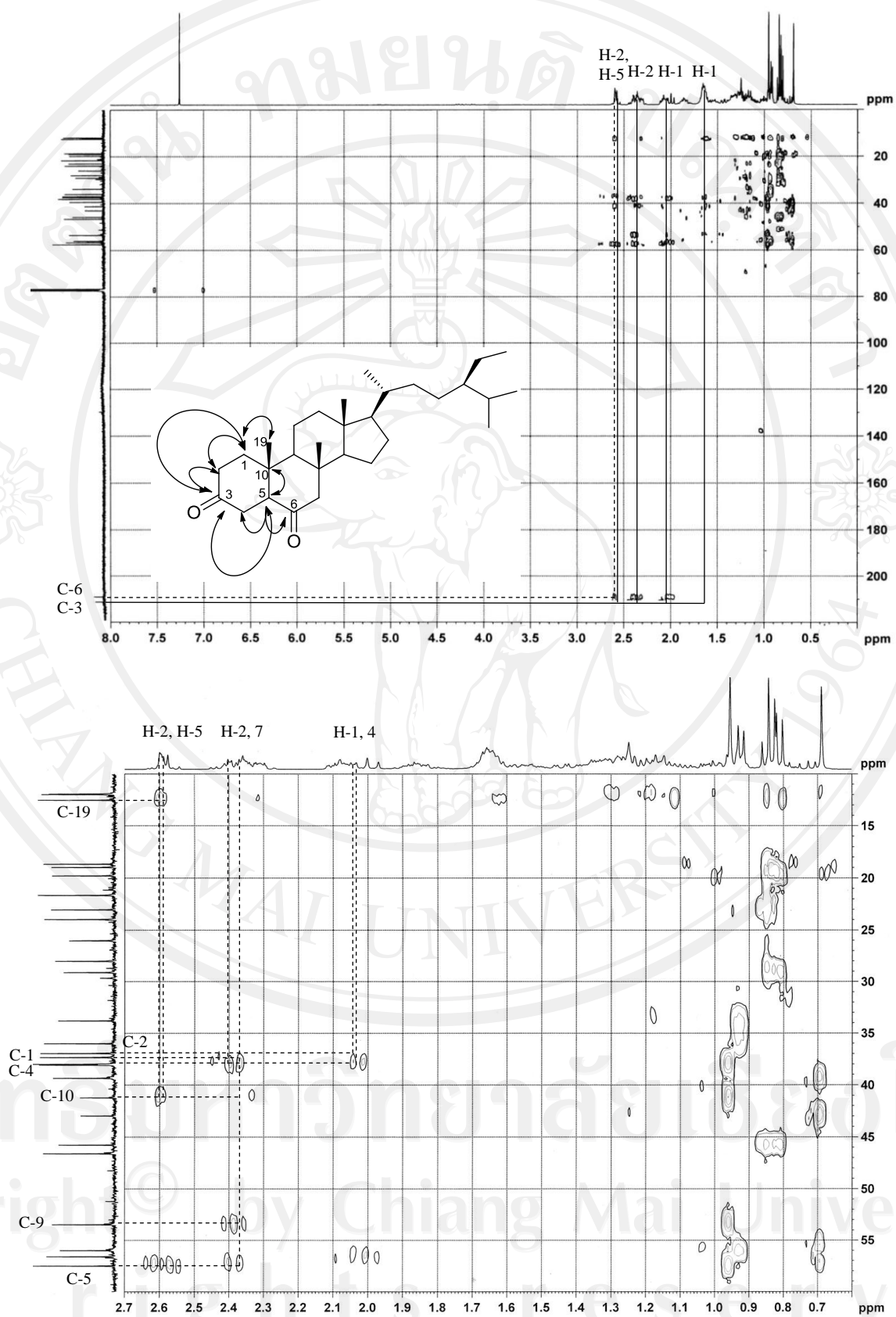
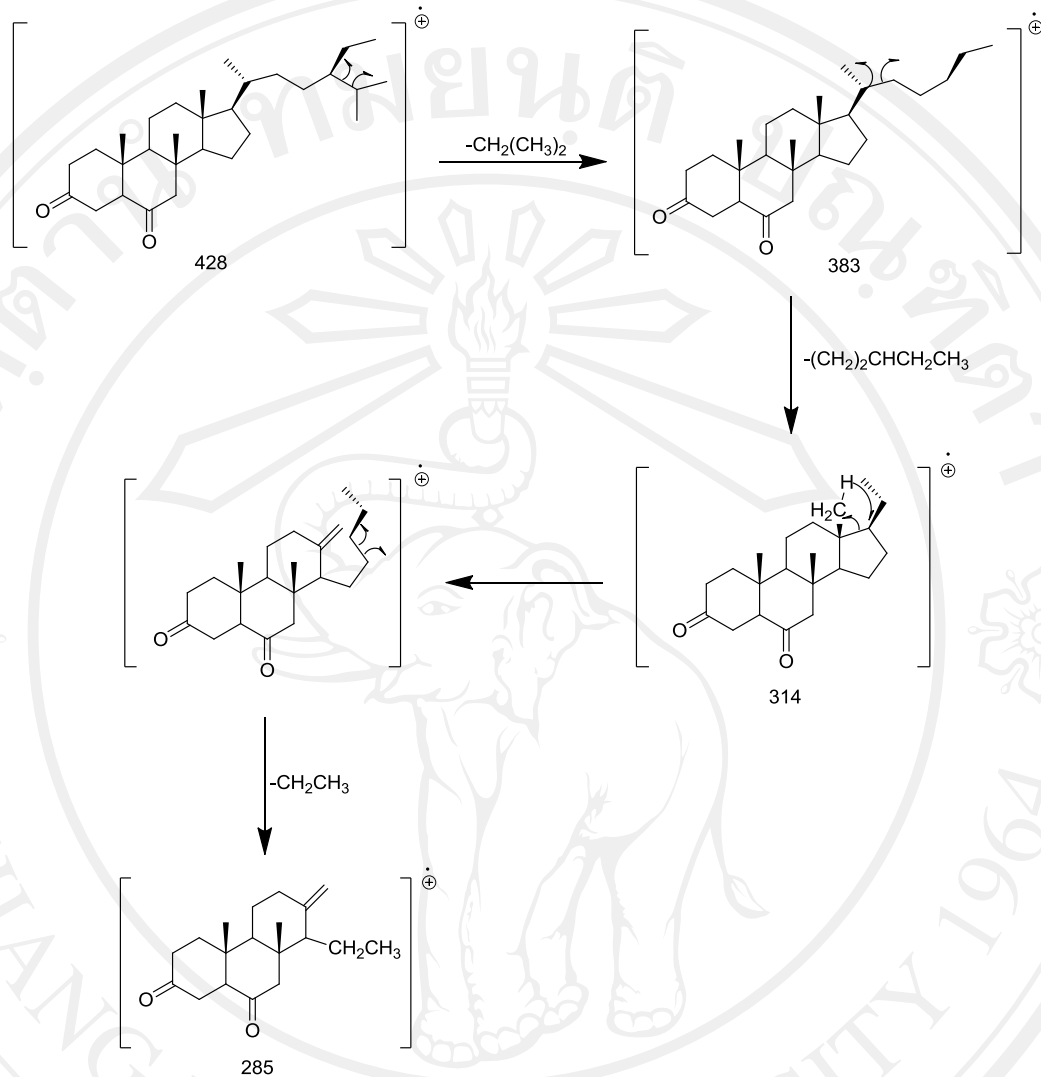


Figure 22 Selected HMBC correlation of stigmastan-3,6-dione (25)

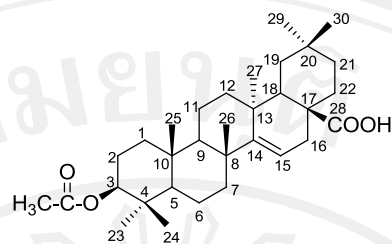


**Figure 23** The fragmentation pathways for stigmastan-3,6-dione (25)

The structure of 3-acetyl aleuritolic acid (**26**) (Figure 24) was elucidated by spectroscopic techniques mainly  $^1\text{H}$  NMR,  $^{13}\text{C}$  NMR, DEPT, COSY, HMQC, HMBC, MS and IR (Figure 25-30, Table 11 and 12). Compound **26**, as furnished white needles, mp 304 – 306°C,  $[\alpha]_{\text{D}}^{29.3} +124.8^\circ$ . The IR spectrum exhibited nearly identical absorption bands of carboxylic acid at 3434, 1733 and 1245  $\text{cm}^{-1}$  attributable to acetoxy group, the C–O–C linkage of ether at 1026  $\text{cm}^{-1}$  moieties and 1689  $\text{cm}^{-1}$  for olefin group.[47, 49]

In the 400 MHz  $^1\text{H}$  NMR (Figure 25), manifested a characteristics singlet at 2.04 ppm assigned to acetoxy protons, a doublet by doublet centered at  $\delta$  5.50 (*d*, H-15,  $J = 7.9, 3.3$  Hz) indicating a proton on a trisubstituted double bond. Another doublet pattern downfield at  $\delta$  4.46 (*d*, H-3,  $J = 11.5, 6.3$  Hz) assigned to the ubiquitous 3  $\alpha$  methane proton germinal to the acetoxy group of triterpenes skeleton. In the region of 0.85-0.98 ppm, seven methyl signals appeared as singlet.

The  $^{13}\text{C}$  NMR spectrum, in combination with DEPT experiments (Figure 26), demonstrated the presence of 32 carbon resonances which composed of seven methyl, ten methylene, five methine and seven quaternary carbons.[49] The signals at 171.0 and 183.6 ppm indicated the presence of carbonyl function of acetoxy and carboxylic acid. The acetyl group was assigned at 80.9 ppm (C-3) due to the presence of the HMBC correlations (Figure 29) between H-3 with carbonyl carbon of the acetyl group at 171.0 ppm and double bond was located at 116.8 and 160.6 ppm, as determined by cross-peaks at 5.50 ppm (H-15) with C-8, C-12 and C-17. Furthermore, the direct C-H bond correlation HMQC technique (Figure 28) was established. It revealed that the C-9, C-15 and C-18 were methine. The exploration of COSY spectrum (Figure 27) allowed us to confirm compound **26** by the observation of H-2, H-3, H-5, H-6 and H-7 in the A and B rings of pentacyclic skeleton. Full assignments of the  $^1\text{H}$  and  $^{13}\text{C}$  NMR signals were accomplished using;  $^1\text{H}$ - $^1\text{H}$  COSY, HMQC and HMBC experiments. This compound is a mono acetoxy pentacyclic triterpenes with mono carboxylic acid and appeared to be identical with the earlier report of 3-acetyl aleuritolic acid.[49-52]

3-acetyl aleuritic acid (**26**)

**Figure 24** Labelling number of each carbon in structure of  
3-acetyl aleuritic acid (**26**)

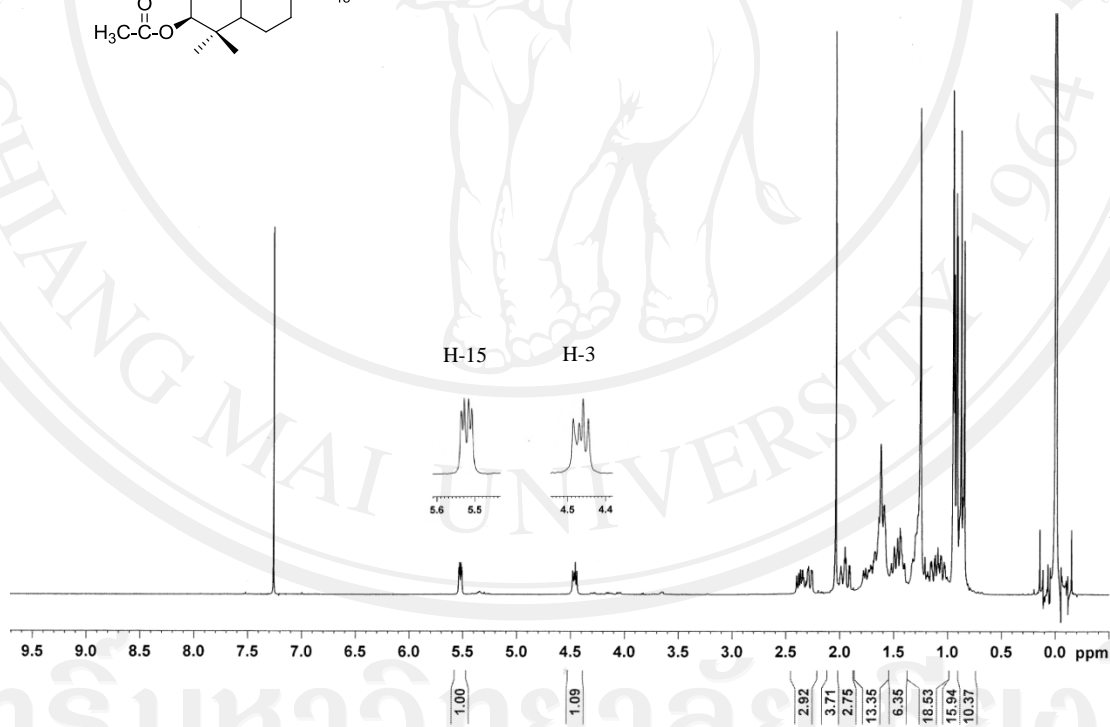
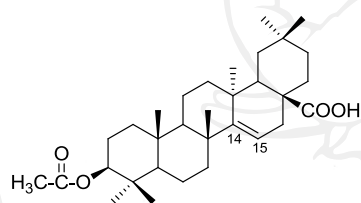


**Figure 25**  $^1\text{H}$  NMR spectrum of 3-acetyl aleuritic acid (**26**)

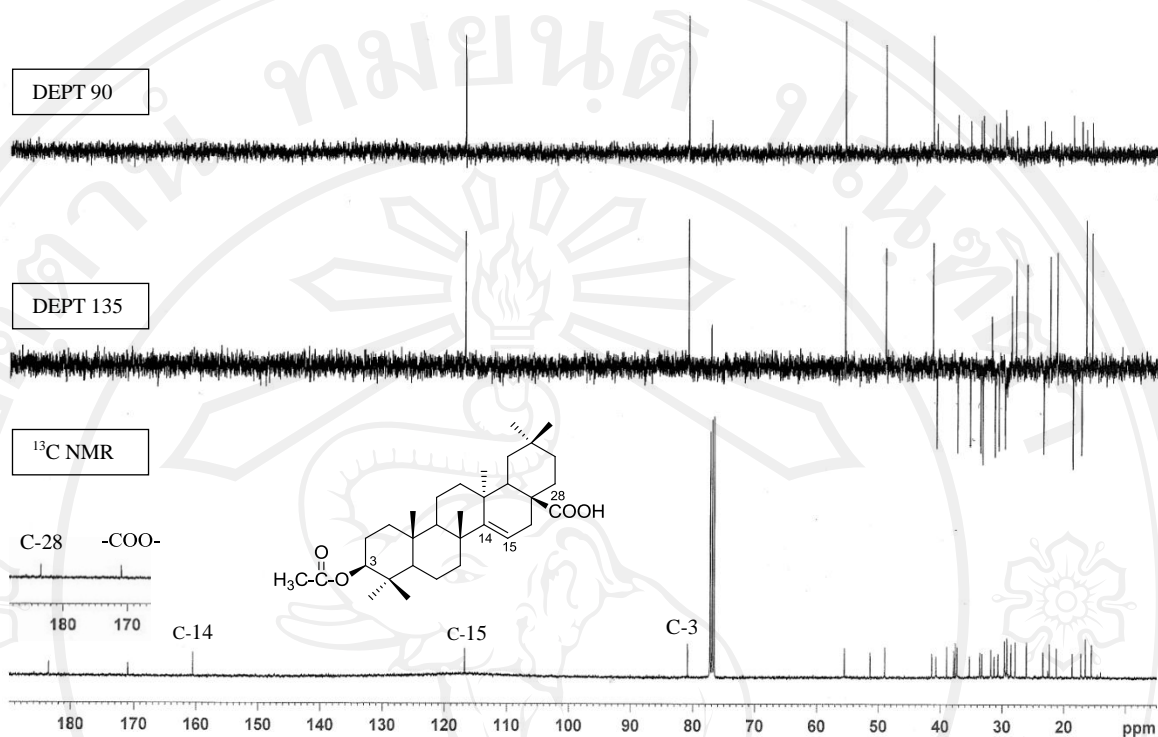


**Figure 26** DEPT 90, DEPT 135 and  $^{13}\text{C}$  NMR spectra of 3-acetyl aleuritolic acid (**26**)

**Table 9**  $^1\text{H}$  and  $^{13}\text{C}$  NMR data of 3-acetyl aleuritolic acid (**26**) ( $\text{CDCl}_3$ ) at 400 MHz ( $^1\text{H}$  NMR) and 100 MHz ( $^{13}\text{C}$  NMR)

Position	Chemical shift ( $\delta$ ) in ppm	
	$^1\text{H}$ NMR	$^{13}\text{C}$ NMR
1	0.99-1.03, 1.59-1.62 [ <i>m</i> , 2H]	37.4
2	1.65, 1.74 [ <i>obsc</i> , 2H]	23.5
3	4.46 [ <i>dd</i> , 1H], $J = 11.5, 6.3$ Hz	80.9
4	-	37.7
5	0.85 [ <i>m</i> , 1H]	55.6
6	0.97, 1.24 [ <i>m</i> , 2H]	18.7
7	1.41-1.44 [ <i>m</i> , 2H]	40.8
8	-	39.0

**Table 9**  $^1\text{H}$  and  $^{13}\text{C}$  NMR data of 3-acetyl aleuritolic acid (**26**) ( $\text{CDCl}_3$ ) at 400 MHz ( $^1\text{H}$  NMR) and 100 MHz ( $^{13}\text{C}$  NMR) (Cont.)

Position	Chemical shift ( $\delta$ ), ppm	
	$^1\text{H}$ NMR	$^{13}\text{C}$ NMR
9	1.39-1.41 [ <i>m</i> , 2H]	49.0
10	-	37.9
11	-	17.3
12	2.26-2.40 [ <i>m</i> , 1H], 1.95 [ <i>t</i> , 1H, $J = 2.9, 3.4$ Hz]	33.3
13	-	37.3
14	-	160.6
15	5.54 [ <i>dd</i> , 1H, $J = 7.9, 3.3$ Hz]	116.8
16	1.69-1.72, 1.91-1.95 [ <i>obsc</i> , 2H]	31.3
17	-	51.4
18	2.27 [ <i>dd</i> , 1H], $J = 2.2, 2.3$ Hz	41.5
19	-	35.3
20	-	29.3
21	1.29 [ <i>obsc</i> , 2H]	33.7
22	1.65 [ <i>obsc</i> , 2H]	37.3
23	0.89 [ <i>s</i> , 3H]	27.9
24	0.85 [ <i>s</i> , 3H]	16.6
25	0.95 [ <i>s</i> , 3H]	15.6
26	0.95 [ <i>s</i> , 3H]	26.2
27	0.92 [ <i>s</i> , 3H]	22.4
28	-	183.6
29	0.93 [ <i>s</i> , 3H]	31.9
30	0.91 [ <i>s</i> , 3H]	28.7
-O <u>C</u> OCH <sub>3</sub>	-	171.0
-O <u>C</u> O <u>C</u> H <sub>3</sub>	2.04 [ <i>s</i> , 3H]	21.3

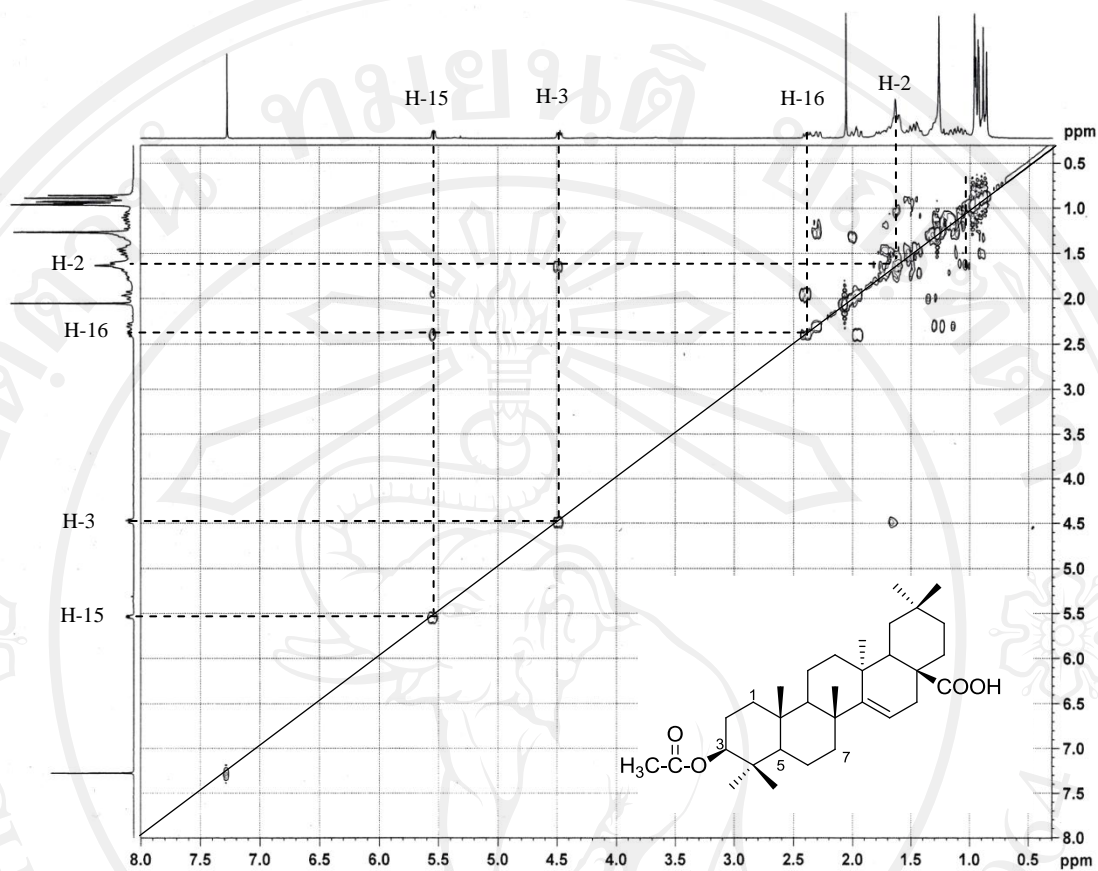
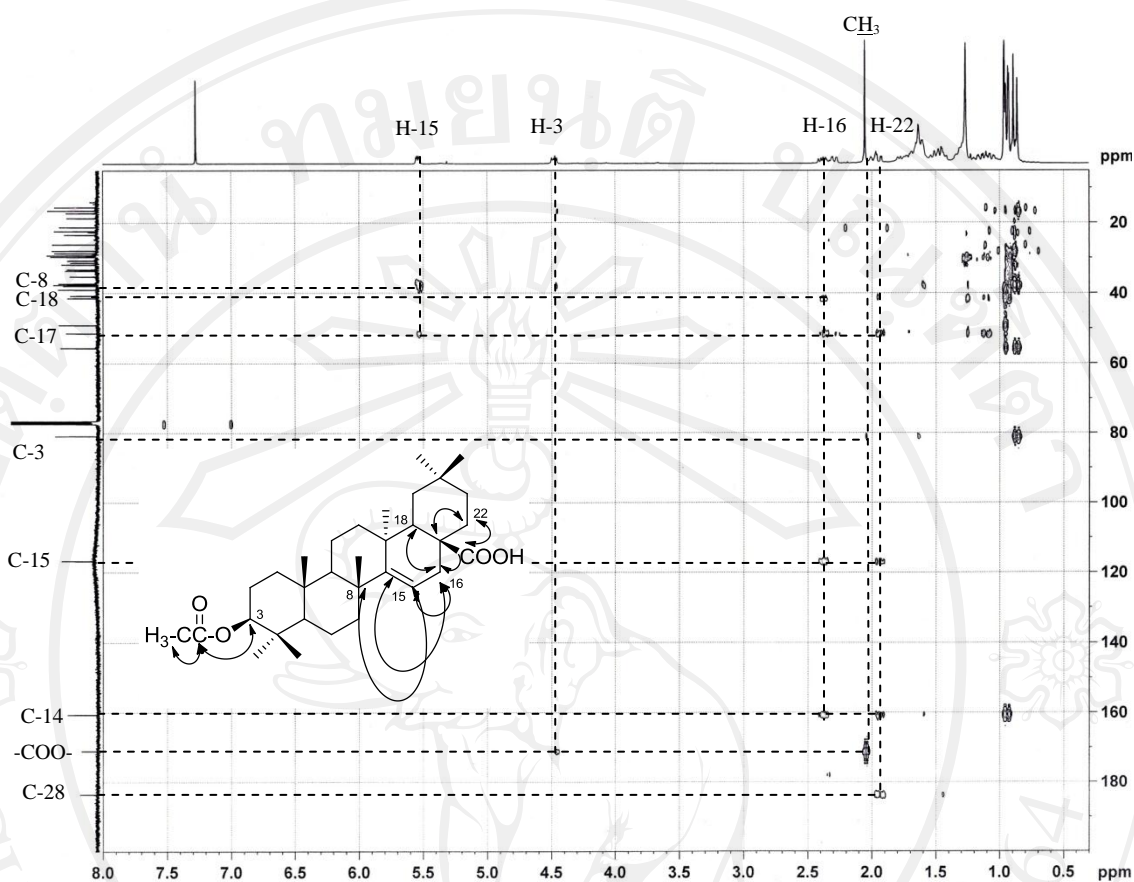
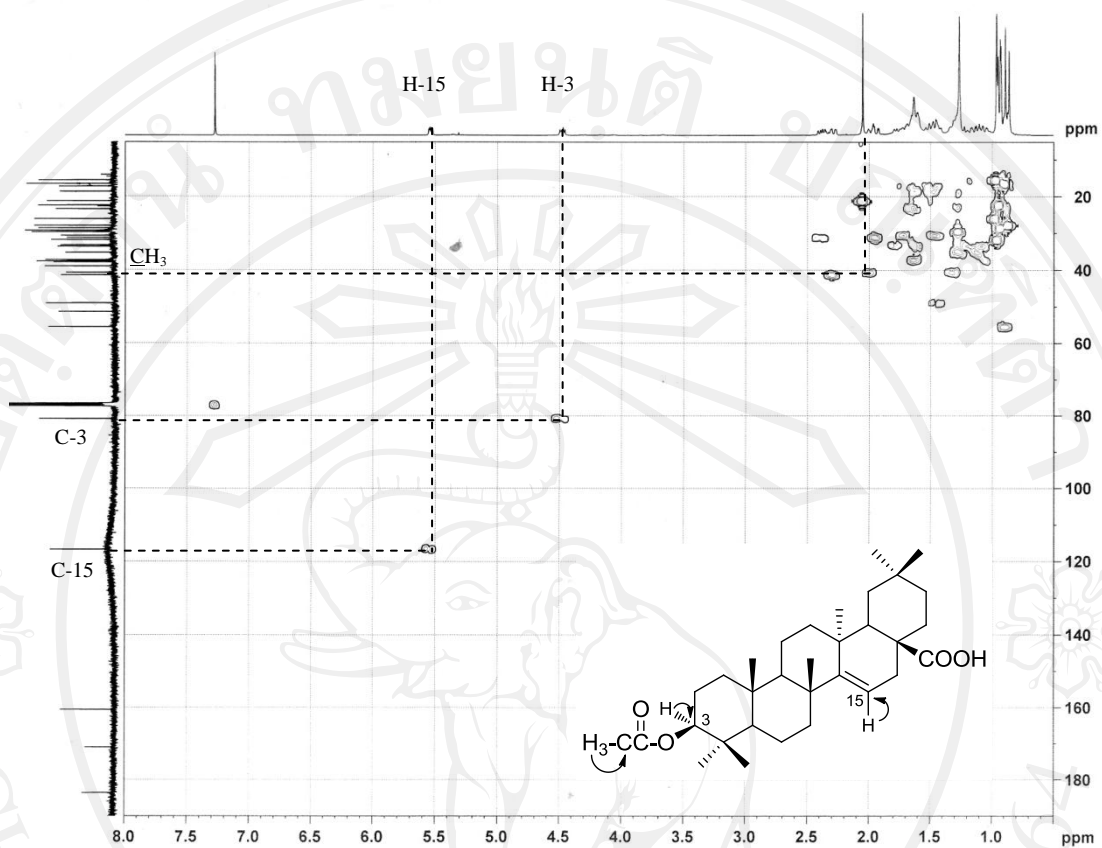


Figure 27  $^1\text{H}$ - $^1\text{H}$  COSY spectrum of 3-acetyl aleuritolic acid (26)



**Figure 28** Selected HMQC correlation of 3-acetyl aleuritolic acid (**26**)



**Figure 29** Selected HMBC correlation of 3-acetyl aleuritolic acid (**26**)

**Table 10**  $^1\text{H}$ - $^1\text{H}$  COSY, HMQC, HMBC data of 3-acetyl aleuritolic acid (**26**) ( $\text{CDCl}_3$ ) at 400 MHz ( $^1\text{H}$  NMR) and 100 MHz ( $^{13}\text{C}$  NMR)

Proton position	$^1\text{H}$ - $^1\text{H}$ COSY (Coupling of H)	HMQC (Correlation of C)	HMBC (Correlation of C)
1	H-2, 5	C-1	C-3, 4
2	H-1, 3	C-2	C-3
3	H-2	C-3	C-2, 4, 6, -OCOCH <sub>3</sub> -OCOCH <sub>3</sub>
4	-	-	C-3, 6
5	H-6	C-5	C-7, 6, 9
6	H-5, 7	C-6	C-24
7	-	-	-
8	-	-	-

**Table 10**  $^1\text{H}$ - $^1\text{H}$  COSY, HMQC, HMBC data of 3-acetyl aleuritic acid (**26**) ( $\text{CDCl}_3$ ) at 400 MHz ( $^1\text{H}$  NMR) and 100 MHz ( $^{13}\text{C}$  NMR) (Cont.)

Proton position	$^1\text{H}$ - $^1\text{H}$ COSY (Coupling of H)	HMQC (Correlation of C)	HMBC (Correlation of C)
9	-	-	-
10	-	-	-
11	-	-	-
12	H-15, 27	C-12	C-14, 15
13	-	-	-
14	-	-	-
15	H-12, 16	C-15	C-8, 12, 17
16	H-15	C-16	C-14, 15, 17, 18
17	-	-	-
18	H-27	C-18	C-13, 19
19	-	-	-
20	-	-	-
21	-	C-21	-
22	-	C-22	C-16, 17, 28
23	-	C-23	C-3, 4, 5
24	-	C-24	C-3, 4, 5
25	-	C-25	C-1, 5, 9, 10
26	-	C-26	C-14
27	-	C-27	C-13, 14, 18, 19
28	-	-	-
29	-	-OCOCH <sub>3</sub>	C-19, 20, 21
30	-	C-30	C-19, 20, 21
-OCOCH <sub>3</sub>	-	-	-
-OCOCH <sub>3</sub>	-	-OCOCH <sub>3</sub>	C-3, -OCOCH <sub>3</sub>

From EI-MS method, the molecular ion peak  $[M^+]$  of this compound was not found in the experiment. However, the other key fragments were observed from mass spectrum at  $m/z$  454, 249, 204 and 189 which was explained the mechanism in previous literature as indicated below Figure 27.[52]

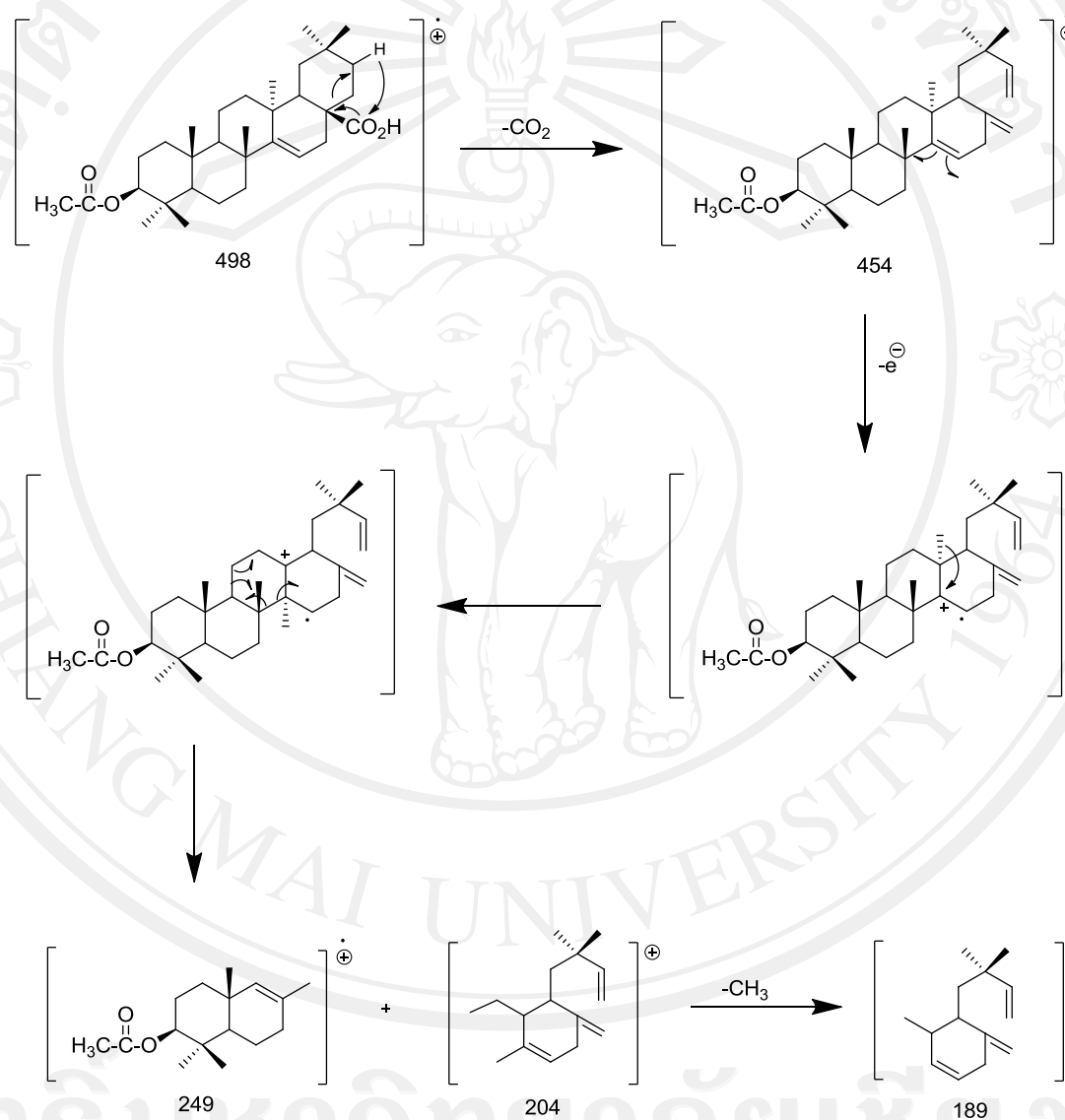


**Figure 30** The fragmentation pathways for 3-acetyl aleuritolic acid (26)

## 4.2 Biosynthesis of isolated compounds

Eugenol (**22**) followed the pathway of shikimic acid pathway and synthesized from shikimic acid via the precursor of phenylalanine and coniferyl alcohol as depicted in Figure 31.[30,31]

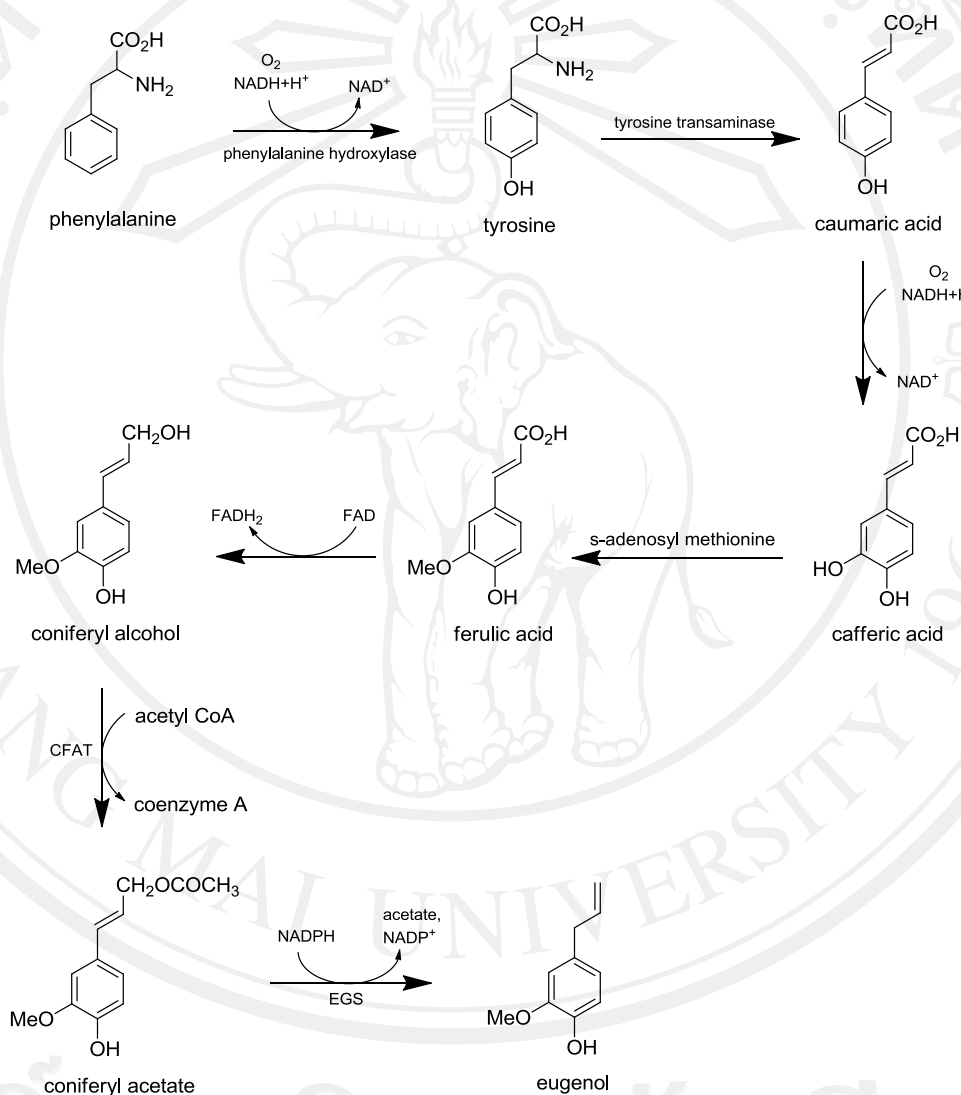


**Figure 31** The biosynthesis of the eugenol (**22**)

$\beta$ -sitosterol (**23**), stigmasterol (**24**) and stigmastan-3,6-dione (**26**) consist of six isoprene units. They derived from five-carbon of isoprenoids, isopentenyl diphosphate (IPP) and dimethylallyl diphosphate (DMAPP) to the formation of the C-30 and originated exclusively from the mevalonate pathway. They are mainly made up of cholesterol and their precursor are lanosterol as seen above in Figure 32.[20, 33, 40]

3-acetyl aleuritic acid (**26**) was pentacyclic triterpenoids. They derived the acetate or mevalonate pathway. The pentacyclic system is generated from squalene in all-chair conformation. Squalene arises from an initial condensation of two molecules of farnesyl diphosphate (FPP) which undergoes a reductive rearrangement to squalene then converted to 2,3-squalene epoxide and by series of concerted cyclization as shown in Figure 33.[47, 51]

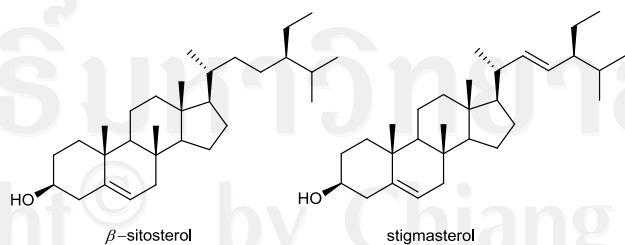
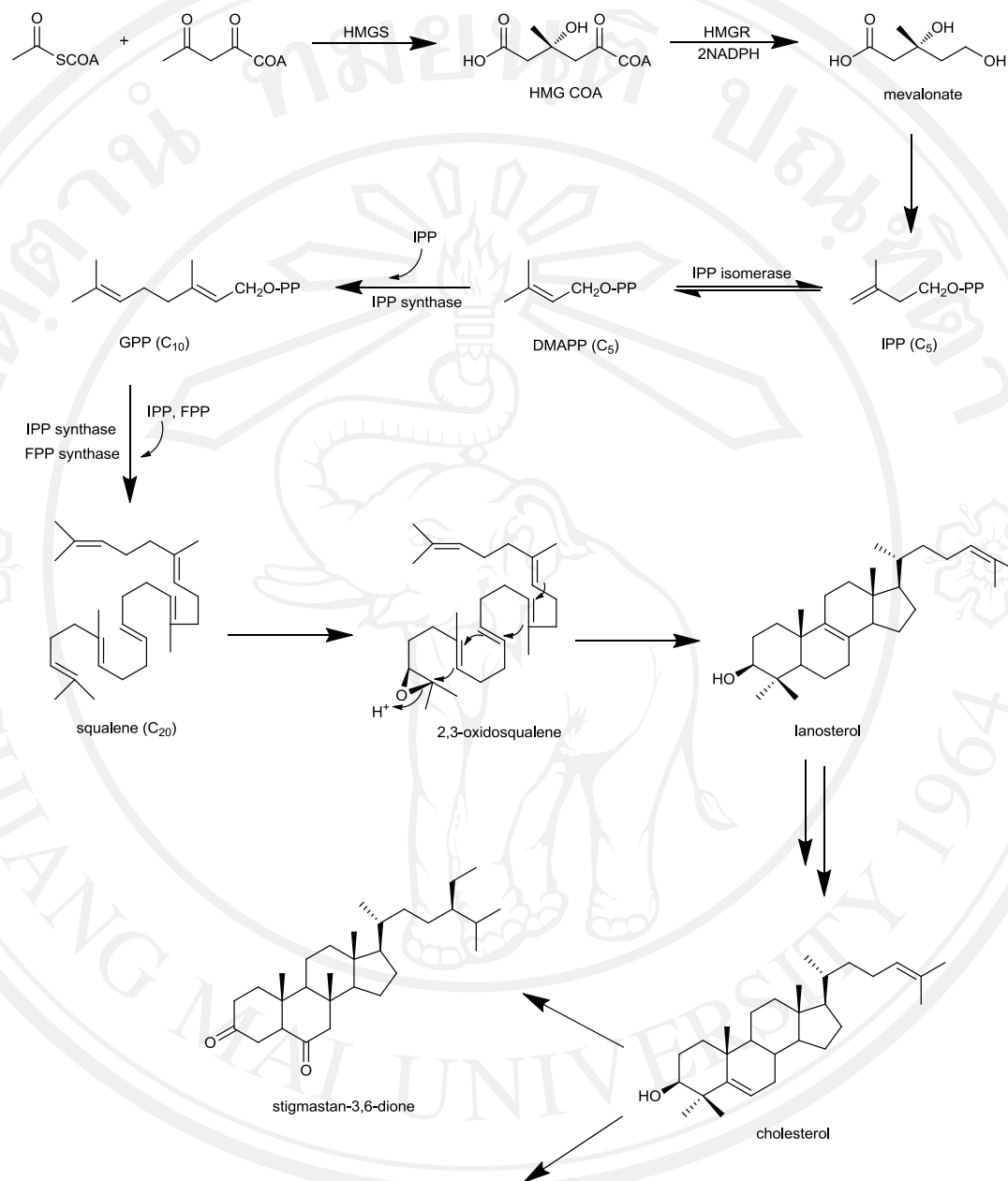


**Figure 32** The biosynthesis of the  $\beta$ -sitosterol (23), stigmasterol (24) and stigmastan-3,6-dione (26)

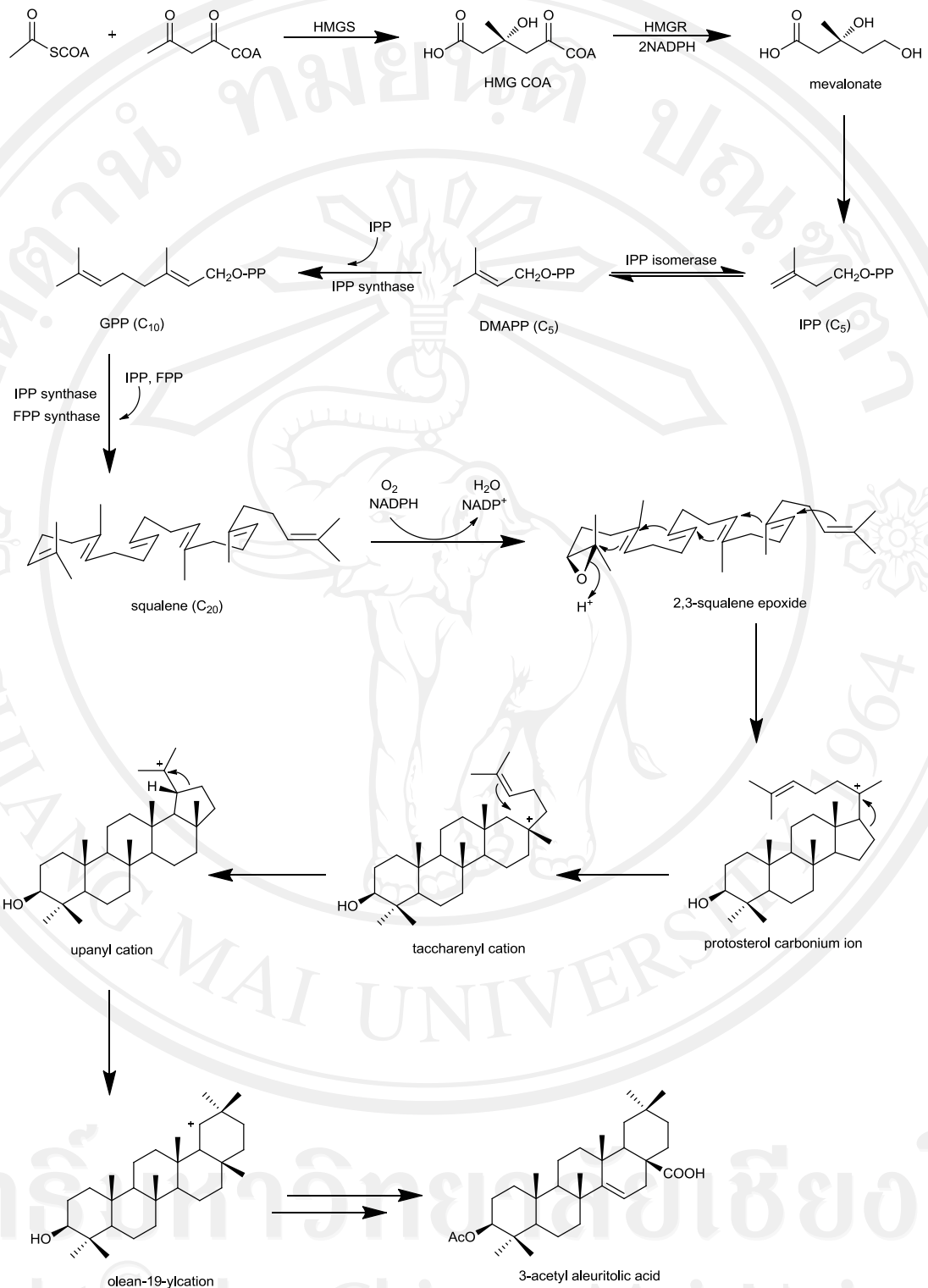


**Figure 33** The biosynthesis of the 3-acetyl aleuritolic acid (26)